Food and Chemical Toxicology 132 (2019) 110657

Contents lists available at ScienceDirect

Food and Chemical Toxicology

journal homepage: www.elsevier.com/locate/foodchemtox

Gastrointestinal digestion of food-use silver nanoparticles in the dynamic SIMulator of the GastroIntestinal tract (simgi®). Impact on human gut microbiota

Carolina Cueva[a], Irene Gil-Sánchez[a], Alba Tamargo[a], Beatriz Miralles[a], Julian Crespo[b], Begoña Bartolomé[a], M. Victoria Moreno-Arribas[a,*]

[a] Institute of Food Science Research (CIAL), CSIC-UAM, C/ Nicolás Cabrera 9, Campus de Cantoblanco, 28049, Madrid, Spain
[b] Departamento de Química. Complejo Científico-Técnico Universidad de La Rioja, C/ Madre de Dios, 51, 26004, Logroño (La Rioja), Spain

ARTICLE INFO

Keywords:
Silver nanoparticles
Simgi® model
Dynamic gastrointestinal digestion
Gut microbiota
AgNPs monitoring and transformation

ABSTRACT

The increasing use of silver nanoparticles (AgNPs) in consumer products has led to concern about their impact on human health. This paper aims to provide new scientific evidence about the modifications and potential effects of AgNPs with food applications during their passage through the digestive tract. For that, two types of AgNPs [solid polyethylene glycol-stabilised silver nanoparticles (PEG-AgNPs 20) and liquid glutathione-stabilised silver nanoparticles (GSH-AgNPs)] were initially subjected to gut-microbial digestion simulation in an *in vitro* static model. Based on these experiments, digestion of GSH-AgNPs was carried out in a dynamic model (simgi®) that simulated the different regions of the digestive tract (stomach, small intestine and the ascending, transverse and descending colon) in physiological conditions. Dynamic transport of GSH-AgNPs in the simgi® was similar to that observed for the inert compound Cr-EDTA, which discarded any alterations in the intestinal fluid delivery due to the AgNPs. Also, feeding the simgi® with GSH-AgNPs seemed not to induce significant changes in the composition and metabolic activity (i.e., proteolytic activity) of the gut microbiota. Concerning monitoring of AgNps, it was observed that the GSH-AgNPs underwent several transformations in the gastrointestinal fluids and appeared to expose the intestine in ways that were structurally different from the original forms. In compliance with European guidelines, the simgi® model can be considered a useful *in vitro* tool to evaluate the effects of nanoparticles at the digestive level, prior to human studies, and, therefore, minimising animal testing.

1. Introduction

Over the past decades, silver nanoparticles (AgNPs) have been defined as food additives and/or food contact materials in consumer products, mostly because of their antimicrobial properties (Chaudhry et al., 2008; Monge and Moreno-Arribas, 2016). Thus, AgNPs have achieved a renewed, increasing, interest due to the search for new antimicrobial alternatives that could replace or complement the action of food chemical preservatives (García-Ruiz et al., 2015; Gil-Sánchez et al., 2019). In this sense, a recent study has demonstrated the potential application of two AgNPs, PEG-AgNPs 20 and a GSH-AgNPs, in controlling microbial process in winemaking (Gil-Sánchez et al., 2019). Silver nanoparticles can be coated to facilitate their interaction with the environment; a coating of glutathione (GSH) increases the solubility and the ability of silver nanoparticles to interact with the environment. GSH-AgNPs have potential applications as antimicrobial agents against the foodborne pathogen *Campylobacter* (Silvan et al., 2018), both in the production and processing of poultry meat or as an alternative to disinfectants in the *Campylobacter* biofilm control. The increasing industrial production of poultry makes highly likely that there is a direct oral exposure of AgNPs and/or silver ions (Ag^{+}) in human populations, for example through the chicken meat (Sergeevna et al., 2018), with an estimated dietary intake of silver is 70–90 μg per day, or even higher (Wijnhoven et al., 2009). Therefore, nanoparticle toxicity is a major concern in the use and development of nanotechnology.

The study of a human digestion process can be addressed with different approaches including *in vitro* to *in vivo* methods. Due to their physiological relevance, investigations with animals and human trials generally offer the most precise results and are still considered the 'gold standard' for determined diet-related questions. Unfortunately, analysis of the complex multistage processes of human digestion is technically complicated, costly and is limited by ethical restrictions (Lucas-

* Corresponding author.
E-mail address: victoria.moreno@csic.es (M.V. Moreno-Arribas).

https://doi.org/10.1016/j.fct.2019.110657
Received 5 March 2019; Received in revised form 29 June 2019; Accepted 1 July 2019
Available online 02 July 2019

González et al., 2018). Consequently, there is a real need for the use of *in vitro* models which mimic the physiological conditions occurring during human digestion. They are also useful tools for studying and understanding changes, interactions and bioaccessibility of nutrients, drugs, and non-nutritive compounds (Lucas-González et al., 2018; Ménard et al., 2014). The main types of *in vitro* systems are static and dynamic models. Static models consist of a series of bioreactors that simulate most of the physiological parameters (pH, temperature, enzyme concentration, etc.) of the different compartments involved in digestion (the mouth, stomach, small and large intestine). However, it is difficult to recreate the complexity of the gastrointestinal tract in these models as they do not simulate the transient biochemical and flow conditions of food travelling through the different compartments in real time, which could have a great impact on the breakdown of larger food particles and the subsequent release of nutrients (Guerra et al., 2012). In contrast, dynamic models are closer to the physiological reality of the entire gastrointestinal tract. These systems allow validate the dynamic environment of the gut providing evidence of influx in body secretions, temperature, peristaltic mixing, pH control, dynamic flows in the different compartments, and, in some cases, the mucosal microbial colonization by incorporation of mucin-covered microcosms (Dupont et al., 2018; Ménard et al., 2014). However, due to its enormous complexity, as well as the high cost of installation and optimisation process, there are very few simulators of this type in the world (Dupont et al., 2018). One of these simulators is the simgi®, a computer-controlled gastrointestinal *in vitro* model designed to simulate the physiological processes taking place during digestion in the stomach and small intestine, while also reproducing the colonic microbiota responsible for metabolic bioconversions in the large intestine (Barroso et al., 2015; Cueva et al., 2015). The studies carried out so far in the simgi® have been focused on different foods (Cueva et al., 2015; Gil-Sánchez et al., 2018; Miralles et al., 2018; Tamargo et al., 2017). However, dynamic simulators like the simgi® have been shown to be useful for other interesting applications such as evaluating the digestion process, bioaccessibility, and the effects on intestinal microbiota of Active Pharmaceutical Ingredients (API) (Brouwers et al., 2011), insecticides (Joly et al., 2013), heavy metals (Sun et al., 2017; Yin et al., 2017) and engineered nanomaterials (Lefebvre et al., 2015).

After ingestion, the AgNPs pass through the gastrointestinal tract where they can undergo morphological and physicochemical modifications (Pindáková et al., 2017). In this sense, Walczak et al. (2012) has been recently demonstrated that the AgNPs size and morphology of changes upon their exposure to saliva, gastric and intestinal fluids and that these changes depend on the composition and the pH of each fluid. The same study reflects that these nanoparticles display low toxicity and inflammatory effects on human tissue models. Another recent study by Kästner et al. (2017) points to aggregation of small size Ag NPs (3 nm) without changes on the size and size distribution of the individual nanoparticles. While the study of these effects using *in vitro* static models have been evaluated in different studies (Catto et al., 2019; Gil-Sánchez et al., 2018; Ramos et al., 2017; Walczak et al., 2012), understanding of AgNPs gut modifications in physiological dynamic systems is very limited. Furthermore, little is known about the role of AgNPs on two emerging players in gut nanotoxicology, the mucus and microbiota. A recent review of work by Mercier-Bonin et al. (2018) highlights the interest of these key factors in intestinal homeostasis and host health as they directly influence the distribution of nanoparticles in the systemic compartment. With the aim of improving the scientific evidence about the modifications and potential effects of silver nanoparticles during their passage through the digestive tract, in this study AgNPs were subjected to gut-microbial digestion simulation in *vitro* static model and to complete gastrointestinal fluid dynamic transport using the simgi® model. Dynamic transport of AgNPs in the simgi® was compared to that of an inert compound Cr-EDTA. Furthermore, changes in microbiota composition (microbial counts and qPCR analysis), microbial metabolic activity (ammonium production), and in AgNPs size, shape, stability, and aggregation were evaluated in the different simgi® compartments (stomach, small intestine, ascending colon, transverse colon, and descending colon) after feeding the system with AgNPs.

2. Materials and methods

2.1. Materials

2.1.1. Chromium (III)-Ethylenediaminetetraacetic acid complex

Chromium (III)-Ethylenediaminetetraacetic acid (also known by Cr-EDTA complex), a non-absorbable and non-hydrolysable water soluble marker (Barbé et al., 2013), was selected as a digestive marker to validate the complete operation of simgi®. This compound was purchased in Sigma-Aldrich (St. Louis, MO).

2.2. Silver nanoparticles

Two biocompatible silver nanoparticles, solid polyethylene glycol-stabilised silver nanoparticles (PEG-AgNPs 20) and liquid glutathione-stabilised silver nanoparticles (GSH-AgNPs) were used in this study. Both were synthesised following the guidelines described by García-Ruiz et al. (2015). The final silver concentration and particle average size were 20% w/w and a main population of ca. 3-5 nm size with some particles between 10-25 nm for PEG-AgNPs 20; and 0.197 mg/ml and a small size population of ca. 4-6 nm and a larger size population between 10–50 nm for GSH-AgNPs. The size histograms for each type of AgNPs are provided in Fig. 1.Nanoparticle size histograms were obtained through the analysis of several TEM micrographs for each sample. The size measurements on a wide population of nanoparticles were performed using ImageJ (v1.44) software. The frecuency count and the histogram graphical representation were obtained using Origin 8.0 software.

2.3. In vitro static fermentations of AgNPs

Fresh faecal samples were collected from three healthy volunteers (#1, #2 and #3) who declared, not to be suffering from any disease or intestinal disorder and had not received antibiotics for at least 6 months before the start of the study. Faeces were collected after a maximum of 2 h from defecation and maintained in anaerobic conditions until the moment of the experiment. A 1:10 (w/v) dilution of the faecal samples with the anaerobic phosphate buffer (0.1 M, pH 7) was prepared and homogenised in a stomacher for 2 min at maximum speed.

Sterilised fermentation flasks were filled with 45 mL of colon nutrient medium containing peptone water (2 g/L), yeast extract (2 g/L), sodium chloride (NaCl) (0.1 g/L), dipotassium phosphate (K_2HPO4) (0.04 g/L), monopotassium phosphate (KH_2PO4) (0.04 g/L), magnesium sulphate ($MgSO_4.7H_2O$) (0.01 g/L), calcium chloride hexahydrate ($CaCl_2.6H_2O$) (0.01 g/L), sodium bicarbonate ($NaHCO_3$) (2 g/L), Tween 80 (2 mL/L), Hemin (0.05 g/L), Vitamin K (10 µl/L), L-cysteine HCl (0.5 g/L), bile salts (0.5 g/L) and distilled water. After filling, each flask was inoculated with 5 mL faecal slurry and silver nanoparticles, PEG-AgNPs 20 and GSH-AgNPs, at a final concentration of 11 µg/mL and 7.6 µg/mL, respectively. These concentrations correspond to the values that these nanoparticles would reach in the intestinal phase after ingestion of 88 µg/ml of PEG-AgNPs 20, and 61 µg/ml of GSH-Ag, as calculated previously (Gil-Sánchez et al., 2019) by the application of the international harmonised methodology (Minekus et al., 2014). The food relevance lies in the fact that these concentrations allow control the growth of some of the microorganisms involved in the winemaking process (García-Ruiz et al., 2015), and therefore could help to reduce chemical additives (such as SO_2) levels in the final wine. Incubation flasks were stored in anaerobic conditions for a period of 48 h, simulating the condition of a human large intestine (37 °C, pH ≈ 6.8). In addition, control incubations containing faecal microbiota in colon

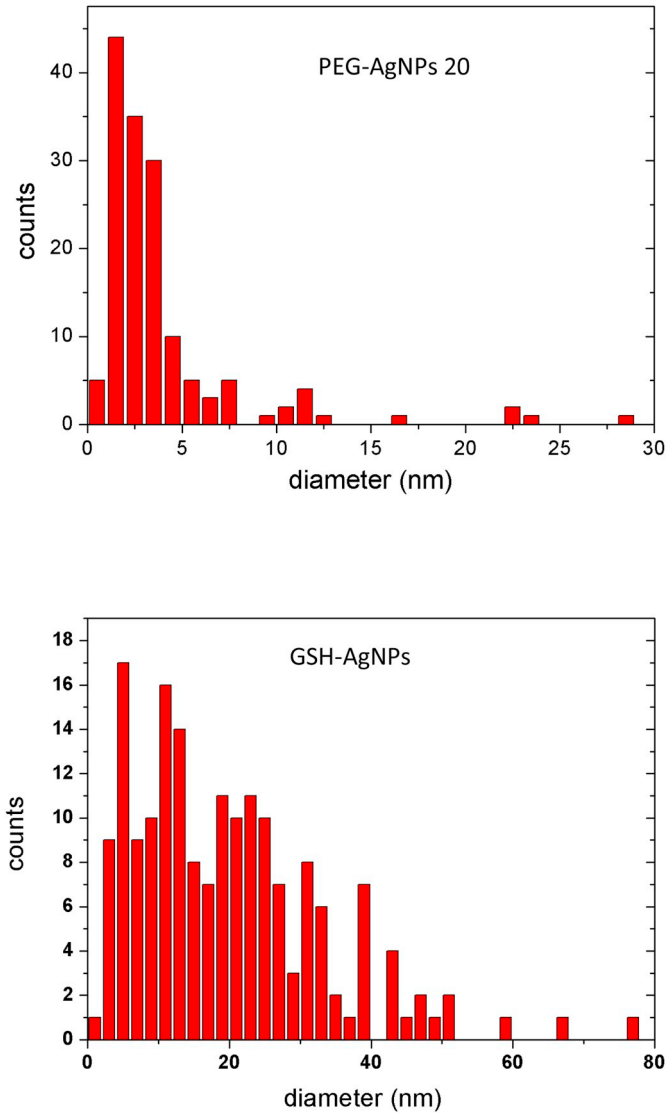

Fig. 1. The size histograms of PEG-AgNPs 20 and GSH-AgNPs.

nutrient medium without silver nanoparticles were also performed. Samples were collected at different incubation times: 0, 10, 24 and 48 h for microbial counting (Section 2.4). Incubations were carried out in triplicate.

2.4. *In vitro dynamical gastrointestinal digestion simulations in the simgi®*

2.4.1. *The in vitro dynamic gastrointestinal simulator (simgi®)*

The simgi® is a computer-controlled gastrointestinal *in vitro* model designed to simulate the physiological processes taking place during digestion in the stomach and small intestine, as well as to reproduce the colonic microbiota responsible for metabolic bioconversions in the large intestine (Barroso et al., 2015; Cueva et al., 2015). The simgi® comprises of five interconnected compartments that simulate the stomach (ST), small intestine (SI), ascending colon (AC), transverse colon (TC), and the descending colon (DC) regions that can operate jointly or independently (Fig. 2). The stomach consists of a cylindrical transparent methacrylate plastic module covering a reservoir of flexible silicone wall, divided into two chambers, where the gastric content is mixed by peristaltic movements. The peristalsis is achieved by changing the pressure of water that flows through the jacket between the plastic modules and the reservoir, this additionally keeps the temperature of the gastric content at 37 °C. The stomach compartment has different ports for input of experimental food components, gastric juice, and acid. The other 4 units (SI, AC, TC and DC) consist of double-jacketed glass reactor vessels continuously stirred at 150 rpm by means of a magnetic stirrer. The intestinal and colonic vessels contain different ports for the transit of intestinal content, sampling points, continuous flushing of nitrogen allowing a permanent anaerobic atmosphere, pH and temperature control. Flow rates, compartment volumes, pH, temperature and pressure are all computer controlled through a programmable logic panel (Unitronics Vision 120TM), additionally, the system stores the on-line monitored values, such as volumes pumped, temperature, and pH throughout the whole experiment.

2.4.2. *Validation of fluid dynamic transport of simgi® using an inert digestion marker*

The parameters of the dynamic gastrointestinal simulation process were selected on the basis of literature data to mimic *in vivo* conditions (Kong and Singh, 2008; Meunier et al., 2008), and preliminary experiments performed with the stomach compartment (Miralles et al., 2018), also with the small intestine-colon combination (Barroso et al., 2015; Cueva et al., 2015; Gil-Sánchez et al., 2018). First, an initial stabilisation period of two weeks was applied to allow the intestinal microbiota to adapt to environmental conditions present in the colon compartments (AC, TC and DC). During this period, the system was fed with nutritive medium containing arabinogalactan (1 g/L), apple pectin (2 g/L), xylan (1 g/L), potato starch (3 g/L), glucose (0.4 g/L), yeast extract (3 g/L), peptone (1 g/L), mucin (4 g/L) and L-cysteine (0.5 g/L).

A summary of selected gastrointestinal parameters is presented in Table 1. At the gastric level, the peristalsis frequency was set to 10 s^{-1}, the food load was 80 ml and the pH curve progressed from 5.6 (pH of the Cr-EDTA complex solution in nutritive medium) to 2 (fasting conditions) during gastric digestion. The pepsin solution was kept in an ice bath to avoid autolysis and was delivered at a 0.5 mL/min flow rate, with a total added volume of 15 ml. The enzymatic activity was determined using haemoglobin as a substrate. To control the gastric emptying, an Elashoff power exponential function was used:

$$y(t) = 2^{-\left(\frac{t}{T_{1/2}}\right)^{\beta}}$$

Where y is the fraction of content delivered to the small intestine, t is the time of delivery, $T_{1/2}$ is the half-life of delivery to the small intestine and β is the factor that describes the shape of the curve (Elashoff et al., 1982; Minekus et al., 1999). The selected Elashoff equation parameters were $T_{1/2}$ = 70 min and β = 0.8 (Kong and Singh, 2008). The emptying gastric content is mixed with 40 ml of the pancreatic juice (5 mL/min) during intestinal digestion (2 h, 37 °C). After that, the content of the vessel was automatically transferred to the following colon compartment (AC) at a flow rate of 5 mL/min, which simultaneously activated the transit of colonic content between the AC, TC and DC compartments at the same flow rate (Barroso et al., 2015). Finally, a washout period of 1 week, feeding the system, with only nutritive medium, was carried out to return to the initial conditions of stabilisation.

After a stabilisation period, and with the aim to validate the operation of complete simgi®, the system was fed with a single dose of Cr-EDTA (0.5 mg/mL). At periodical points of the study, samples (5 ml) from all compartments (ST: at the end of gastric digestion, SI: during intestinal digestion, AC, TC and DC: after the fluid transport between the colonic compartments) were collected: at day 1 (digestion marker feeding), and at days 2, 3, 4, 5 and finally at day 8 (washout period: during this period the system was only fed with nutritive medium). The aliquots for determining the chromium (Cr) concentration by ICP-MS was centrifuged at 10000 rpm for 10 min at 4 °C and stored at −20 °C. Microbial plate count analyses were performed at the time of the sample collection.

Fig. 2. Scheme of simgi® components: stomach (A), machine (B), water bath (C), small intestine (D), ascending colon (E), transverse colon (F), descending colon (G) and pH, T[a] and nitrogen controller's boxes.

Table 1
Simgi® gastrointestinal parameters used during simulation with Cr-EDTA digestive marker.

Stomach		Colon	
Volume ingested	80 ml		
Peristalsis frequency	10 s	*Ascending colon*	
Temperature	37 °C	Initial volume	250 ml
pH acidification profile (min)		Temperature	37 °C
0	5.6	pH	5,6
5	5	Agitation speed	150 rpm
30	4		
45	3.5		
60	3	*Transverse colon*	
70	2	Initial volume	400 ml
Gastric juice (pepsin)	15 ml, 0.5 ml/min	Temperature	37 °C
Gastric emptying		pH	6,3
$t_{1/2}$	70	Agitation speed	150 rpm
β	0,8		
Initial volume	120 ml		
Small intestine		*Descending colon*	
Initial volume	150 ml	Initial volume	300 ml
Temperature	37 °C	Temperature	37 °C
pH	7	pH	6,8
Agitation speed	150 rpm	Agitation speed	150 rpm
Pancreatic juice	40 ml (5 ml/min)		
Digestion time	120 min	Intestinal transit	145 ml (5 ml/min)

2.4.3. *In vitro dynamical gastrointestinal digestion of AgNPs in the simgi®*

Two independent simgi® experiments were conducted, using faecal samples from the same two selected volunteers (#1 and #2) than in static *in vitro* experiments (Section 2.2), minimizing in this way inter-individual differences in gut microbiota. As previously described, a stabilisation period of 2 weeks was applied for both experiments. After this period, and using the same parameters described in section 2.3.2, the system was fed with a single dose of GSH-AgNPs (15.25 μg Ag/mL). As with the static experiments, the selection of the initial dose was based on the content of silver that would be observed in the gastric phase (Gil-Sánchez et al., 2019) after the application of the harmonised protocol (Minekus et al., 2014). Later, a washout period of eight days, feeding the system with nutritive medium only, was carried out.

Samples from all compartments (ST, SI, AC, TC and DC) were specifically collected after the following periods: at day 1 (acute silver nanoparticles feeding), and at days 2, 3, 4, 5 and 8 (washout period). Microbial plate count analyses were performed at the time of the sample collection. The aliquots for silver (Ag) monitoring were autoclaved, whilst the samples collected for ammonium determination were centrifuged at 10000 rpm for 10 min at 4 °C and stored at −20 °C until ready for analysis. Pellets were stored at −80 °C until further analysis of total bacteria and *Lactobacillus* spp. group by qPCR was carried out.

2.5. *Bacterial enumeration*

Decimal dilutions of *in vitro* fermentation and simgi® samples in physiological solution (NaCl 0.9%) were plated on general media: Wilkins-Chalgren agar (BD) for total anaerobes, TSA (BD) for total aerobes; and on selective media: *Clostridium* (Pronadisa) for *Clostridium* spp, MRS (Pronadisa) for lactic acid bacteria, MacConkey agar (BD) for *Enterobacteriaceae* Enterococcus agar (BD) for *Enterococcus* spp., and LAMVAB for specific faecal *Lactobacillus* spp. TSA and LAMVAB plates were incubated at 37 °C in aerobic conditions for 24 h. The other media were incubated at 37 °C in an anaerobic cabinet (BACTRON Anaerobic/Environment Chamber, SHELLAB) for 24 h (Wilkins-Chalgren and MacConkey media) and 48 h (MRS, Enterococcus and TSC media). Results were expressed as colony-forming units (CFU) per millilitre.

2.6. *Determination of metal concentration in simgi® digests*

Samples (0.5 ml) were digested at high pressure in a mixture of 8 ml of nitric acid (HNO_3) 65% and 2 ml of hydrogen peroxide (H_2O_2) 30% in an MLS Ethos 1600 URM Milestone microwave digester, following the protocol described by Zuluaga et al. (2011). Aliquots of the different samples were analysed by inductively coupled plasma mass spectrometry (ICP-MS) using a NexION 300 ICP-MS (PerkinElmer SCIEX™, United States). Samples, in liquid form, were transported by means of a peristaltic pump to a nebuliser system where they were transformed into an aerosol by the action of argon gas. This aerosol was directed to the ionisation zone, where a plasma had been generated by subjecting a flow of argon gas within an oscillating magnetic field induced by a high-frequency current. Under these conditions, the atoms present in

Table 2
Average plate count measurement (± SD) of the three replicates from the three volunteers (static colonic fermentations), expressed in log CFU/mL, at each fermentation time (0–48 h). Paired *t*-test was used to compare differences among the samples (treatment vs. control). Mean values were significantly different from those for the control group: *P < 0.05.

Bacterial group	Volunteers	Treatment	Incubation time (hours)				
			0	5	10	24	48
Total anaerobes	1	PEG-20 AgNPs	8.20 ± 0.08	8.07 ± 0.10	8.49 ± 0.06	8.45 ± 0.04	8.33 ± 0.01
		GHS AgNPs	8.10 ± 0.14	7.70 ± 0.14	8.36 ± 0.08	8.46 ± 0.11	8.48 ± 0.03
		Control	7.84 ± 0.09	7.51 ± 0.19	8.53 ± 0.04	8.43 ± 0.07	8.51 ± 0.03
	2	PEG-20 AgNPs	6.57 ± 0.13	7.45 ± 0.21	8.11 ± 0.05	8.49 ± 0.06	8.32 ± 0.03
		GHS AgNPs	6.68 ± 0.20	8.14 ± 0.09	8.14 ± 0.09	8.43 ± 0.07	8.34 ± 0.19
		Control	6.72 ± 0.08	7.84 ± 0.09	8.41 ± 0.00	8.48 ± 0.04	8.54 ± 0.09
	3	PEG-20 AgNPs	7.54 ± 0.02	7.49 ± 0.10	8.20 ± 0.08	7.05 ± 0.21	7.96 ± 0.26
		GHS AgNPs	7.70 ± 0.07	7.57 ± 0.10	8.32 ± 0.09	7.49 ± 0.10	8.12 ± 0.31
		Control	7.60 ± 0.03	7.47 ± 0.24	8.30 ± 0.00	7.53 ± 0.00	8.14 ± 0.09
Total aerobes	1	PEG-20 AgNPs	5.95 ± 0.01	5.29 ± 0.12	8.25 ± 0.07	8.45 ± 0.00	8.50 ± 0.08
		GHS AgNPs	5.44 ± 0.13	5.27 ± 0.10	8.30 ± 0.06	8.19 ± 0.27	8.53 ± 0.00
		Control	5.37 ± 0.16	5.25 ± 0.07	8.34 ± 0.27	7.87 ± 0.55	8.39 ± 0.12
	2	PEG-20 AgNPs	5.84 ± 0.09	6.95 ± 0.49	8.22 ± 0.11	8.41 ± 0.10	8.32 ± 0.09
		GHS AgNPs	5.45 ± 0.21	6.75 ± 0.21	8.32 ± 0.03	8.43 ± 0.02	8.20 ± 0.08
		Control	5.78 ± 0.00	6.60 ± 0.00	8.41 ± 0.03	8.34 ± 0.11	8.36 ± 0.03
	3	PEG-20 AgNPs	4.60 ± 0.00	4.75 ± 0.21	6.36 ± 0.08	6.93 ± 0.21	7.02 ± 0.17
		GHS AgNPs	4.54 ± 0.34	4.68 ± 0.11	6.30 ± 0.03	7.43 ± 0.02	7.30 ± 0.03
		Control	4.60 ± 0.01	4.69 ± 0.12	6.38 ± 0.05	7.41 ± 0.05	7.32 ± 0.09
Enterobacteriaceae	1	PEG-20 AgNPs	5.49 ± 0.06	4.47 ± 0.12	7.15 ± 0.21	7.72 ± 0.14	7.99 ± 0.07
		GHS AgNPs	5.49 ± 0.02	4.85 ± 0.35	7.06 ± 0.40	7.78 ± 0.02	8.04 ± 0.07
		Control	5.22 ± 0.11	4.04 ± 0.06	7.04 ± 0.37	7.34 ± 0.11	8.05 ± 0.08
	2	PEG-20 AgNPs	5.25 ± 0.36	4.35 ± 0.14	6.90 ± 0.00	7.10 ± 0.14	7.60 ± 0.14
		GHS AgNPs	5.13 ± 0.18	3.84 ± 0.09	7.20 ± 0.00	6.90 ± 0.00	7.13 ± 0.18
		Control	5.15 ± 0.00	4.02 ± 0.17	7.14 ± 0.09	7.02 ± 0.17	7.60 ± 0.06
	3	PEG-20 AgNPs	6.35 ± 0.29	6.74 ± 0.11	5.84 ± 0.08	6.57 ± 0.13	7.05 ± 0.07
		GHS AgNPs	6.35 ± 0.28	6.86 ± 0.01	5.80 ± 0.03	7.02 ± 0.17	6.45 ± 0.21
		Control	6.35 ± 0.28	6.85 ± 0.00	5.72 ± 0.11	7.28 ± 0.03	7.32 ± 0.03
Clostridium spp.	1	PEG-20 AgNPs	7.52 ± 0.20	7.14 ± 0.09	7.57 ± 0.02	7.38 ± 0.18	7.54 ± 0.23
		GHS AgNPs	7.40 ± 0.02	7.43 ± 0.07	7.44 ± 0.09	7.49 ± 0.01	8.62 ± 0.03*
		Control	7.41 ± 0.21	7.13 ± 0.18	7.45 ± 0.27	7.52 ± 0.02	7.55 ± 0.10
	2	PEG-20 AgNPs	7.25 ± 0.07	7.07 ± 0.10	8.43 ± 0.18	8.24 ± 0.14	8.49 ± 0.06
		GHS AgNPs	6.57 ± 0.21	6.45 ± 0.21	8.46 ± 0.02	8.36 ± 0.08	8.53 ± 0.00
		Control	6.69 ± 0.12	6.45 ± 0.21	8.54 ± 0.02	8.58 ± 0.14	8.50 ± 0.17
	3	PEG-20 AgNPs	6.23 ± 0.04	5.65 ± 0.07	6.78 ± 0.00	6.95 ± 0.07	7.19 ± 0.16
		GHS AgNPs	7.20 ± 0.08	5.67 ± 0.01	6.65 ± 0.49	7.05 ± 0.13	7.23 ± 0.04
		Control	6.02 ± 0.17	5.60 ± 0.06	6.69 ± 0.12	7.39 ± 0.20	7.30 ± 0.06
Lactic acid bacteria	1	PEG-20 AgNPs	6.99 ± 0.12	6.34 ± 0.27	6.65 ± 0.23	6.54 ± 0.23	6.43 ± 0.02
		GHS AgNPs	7.18 ± 0.04	6.34 ± 0.19	7.02 ± 0.08	6.59 ± 0.08	6.36 ± 0.08
		Control	7.32 ± 0.03	6.62 ± 0.06	6.84 ± 0.09	6.32 ± 0.09	6.45 ± 0.04
	2	PEG-20 AgNPs	6.11 ± 0.05	6.65 ± 0.04	7.00 ± 0.03	7.04 ± 0.06	6.90 ± 0.43
		GHS AgNPs	6.36 ± 0.08	6.62 ± 0.03	6.75 ± 0.21	6.87 ± 0.38	6.56 ± 0.03
		Control	6.40 ± 0.02	6.60 ± 0.17	7.15 ± 0.07	6.78 ± 0.00	6.39 ± 0.20
	3	PEG-20 AgNPs	6.48 ± 0.04	4.54 ± 0.34	5.84 ± 0.34	5.65 ± 0.13*	5.79 ± 0.09*
		GHS AgNPs	4.72 ± 0.60	4.69 ± 0.55	6.13 ± 0.18	6.60 ± 0.03	6.68 ± 0.05
		Control	5.14 ± 0.09	4.75 ± 0.21	6.34 ± 0.11	6.55 ± 0.14	6.68 ± 0.10
Enterococcus spp.	1	PEG-20 AgNPs	5.17 ± 0.12	5.46 ± 0.02	5.99 ± 0.30	5.89 ± 0.16	5.63 ± 0.04
		GHS AgNPs	5.64 ± 0.08	5.43 ± 0.18	6.43 ± 0.07	6.23 ± 0.21	5.72 ± 0.01
		Control	5.78 ± 0.07	5.14 ± 0.09	6.47 ± 0.08	6.08 ± 0.25	5.56 ± 0.03
	2	PEG-20 AgNPs	5.45 ± 0.04	6.30 ± 0.04	6.84 ± 0.09	7.21 ± 0.29	6.89 ± 0.03
		GHS AgNPs	5.17 ± 0.24	6.69 ± 0.12	6.60 ± 0.04	6.90 ± 0.03	6.75 ± 0.05
		Control	5.34 ± 0.11	6.69 ± 0.12	6.69 ± 0.12	6.84 ± 0.09	6.54 ± 0.09
	3	PEG-20 AgNPs	4.00 ± 0.00	5.36 ± 0.03	6.54 ± 0.02	5.67 ± 0.09*	5.62 ± 0.06*
		GHS AgNPs	3.65 ± 0.49	5.11 ± 0.05	6.95 ± 0.03	6.80 ± 0.11	6.55 ± 0.10
		Control	3.75 ± 0.21	5.24 ± 0.14	6.94 ± 0.04	6.96 ± 0.08	6.57 ± 0.02

*The final silver concentration added to the incubations in static condition was 11 and 7.6 μg Ag/mL for PEG-20 and GHS AgNPs respectively.

the samples were ionised. The ions passed into the quadrupole through an interface of increasing vacuum, where they were separated according to their charge/mass ratio, the separated masses then arrived at a detector where their abundance was determined (Balcaen et al., 2015). This determination was completed by the SIdI analytical service of the Universidad Autónoma de Madrid (UAM) (Spain). This analytical laboratory is certified under the ISO 9001:2000 by AENOR and IQNet.

2.7. Microbiota analysis by quantitative polymerase chain reaction (qPCR) in simgi® digests

Bacterial DNA extraction from pellets of simgi® samples was performed using the QIAamp DNA Stool Mini Kit (Quiagen, Hilden, Germany), following the manufacturer's instructions.

The amplification and detection of the bacterial DNA were carried out on the Applied Biosystems® *ViiA™ 7* Real-Time PCR System using 384-well plates. Each amplification reaction was carried out in duplicate in a final volume of 10 μL that contained 5 μL of SYBER® Select Master Mix (Life Technologies, TX, USA), 0.3 μL of each primer

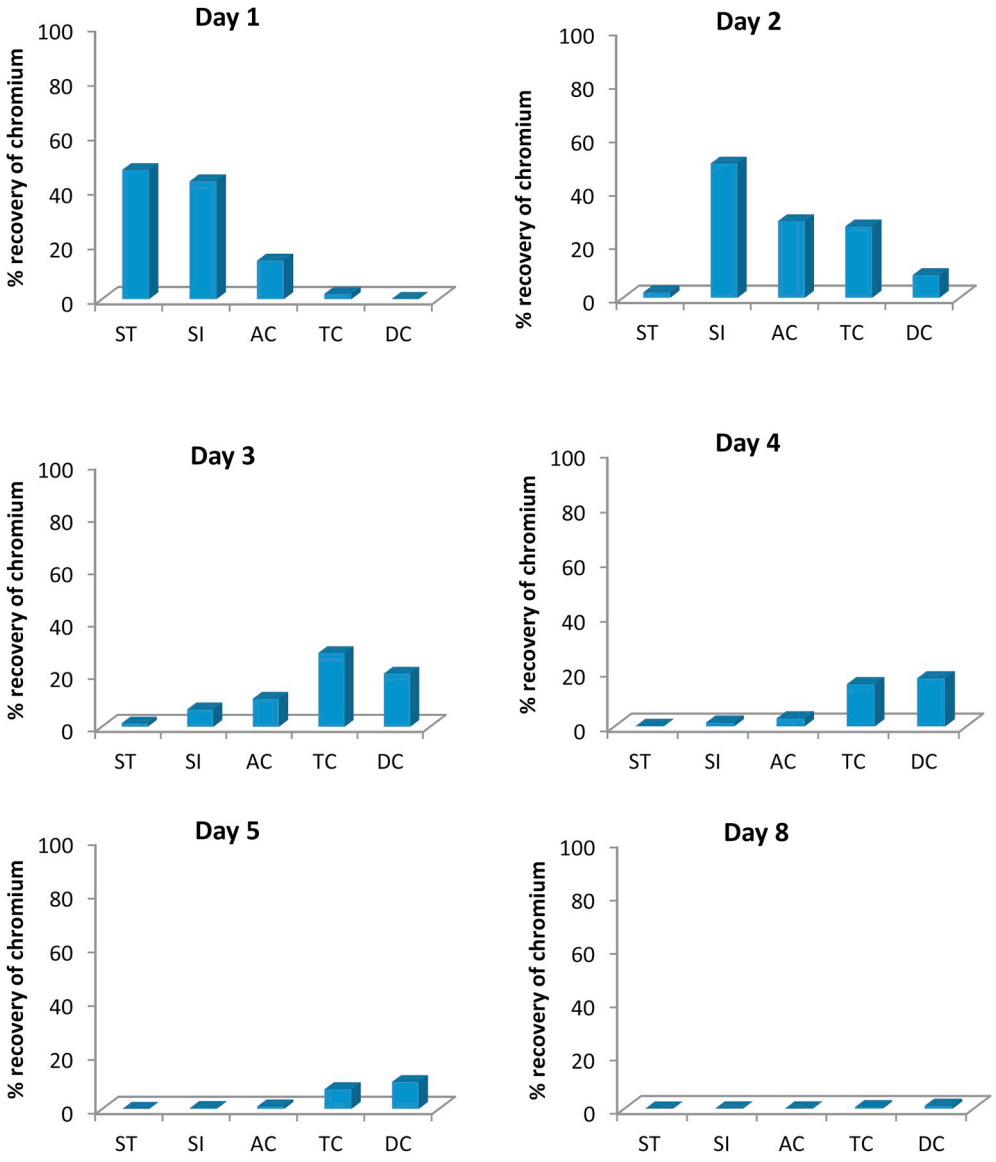

Fig. 3. Evolution of the Cr content in the different simgi® compartments (ST: stomach; SI: small intestine; AC: Ascending Colon; TC: Transverse Colon; and DC: Descending Colon) after a single dose of Cr-EDTA.

(10 μM), 3.4 μL of nuclease-free water purified for PCR (Sigma-Aldrich) and 1 μL of a DNA template. The amplification program consisted of one cycle at 95 °C for 10 min, followed by 40 cycles at 95 °C for 15 s, and 1 min at the appropriate primer-paired temperature (60 °C). The specific primers used in this study were F:GAGAGGAAGGTCCCCCAC and R:CGCKACTTGGCTGGTTCAG for 'total bacteria', and F:AGCAGT AGGGAATCTTCCA and R:CATGGAGTTCCACTGTCCTC for *Lactobacillus* group. Microorganisms used for performing standard curves (*Bacteroides thetaiotaomicron* DSMZ 2079 and *Lactobacillus plantarum* CECT 748) were grown overnight in an MRS broth at 37 °C under anaerobic conditions. Bacterial DNA quantity was expressed as a logarithm of colony-forming units per millilitre (log CFU/mL).

2.8. Ammonium determination in simgi® digests

Ammonium levels were determined using the Ammonium test (Spectroquant Ammonium Test, Merck), following the manufacturer's instructions. Initially, serial dilutions of an ammonium standard solution (10 g/L) were used to prepare calibration curves. Simgi® samples were diluted with deionised water (1:10). Just prior to performing the measurement at 25 °C, 5 ml of reactive NH_4-1 and reactive NH_4-2 were added to the diluted standards and samples. The mixture was shaker between each reagent addition. Then, the absorbance was measured at 690 nm. Analyses were performed in duplicate. The results were expressed as mg of NH_4^+ contained in each colon compartment.

2.9. Analysis of simgi® digests by transmission electron microscopy (TEM)

TEM was used to monitor the presence of remaining nanoparticles in solution and the possible changes exerted on the size, shape, stability and aggregation state of the nanoparticles by the simgi® digestion. TEM samples were prepared by the addition of several drops of centrifuged and filtered digested samples onto carbon-coated copper grids at each stage of the process. TEM images were collected on a JEOL JEM 2100 microscope.

2.10. Statistical analysis

A paired-samples *t*-test was conducted to assess the impact of the silver nanoparticles treatment on different bacterial groups at the same time as the static fermentations. Analysis of variance (one-way ANOVA) was applied to study the effect of GSH-AgNPs' exposure on intestinal

microbiota composition (counts and qPCR data) at day 1 (feeding day) and 2, 3, 4, 5 and 8 (washout period). The least significant differences were calculated by Tukey's test ($p < 0.05$). These analyses were completed using the IBM SPSS Statistics for Windows, Version 23.0; Armonk, NT: IBM Corp).

3. Results

3.1. Experiments in an in vitro static model

Both types of AgNPs [solid polyethylene glycol-stabilised silver nanoparticles (PEG-AgNPs 20) and liquid glutathione-stabilised silver nanoparticles (GSH-AgNPs)] were initially subjected to fermentation with faecal microbiota from three healthy volunteers (#1, #2 and #3) in static conditions. Table 2 depicts the counts of representative bacterial groups (total anaerobes, total aerobes, *Enterobacteriaceae*, *Clostridium* spp., lactic acid bacteria and *Enterococcus* spp.)at different times of the incubation period (0, 5, 10, 24 and 48 h). In general, no significant changes relative to the control were observed in any bacterial groups for both nanoparticles (PEG-20 AgNPs and GSH-AgNPs). Of interest, there was a significant increase ($P \geq 0.05$, $\Delta\log \geq 1$) in the *Clostridium* spp. group for volunteer #1 during the treatment with GSH AgNPs at time point 48 h. The PEG-20 AgNPs induced a decrease in lactic acid bacteria and *Enterococcus* spp. for volunteer #3, times 24 and 48 h (Table 2).

3.2. Experiments in the dynamic SIMulator of the GastroIntestinal tract (simgi®)

3.2.1. Cr-EDTA as a marker of simgi® dynamic transport

Prior to the simulation experiments with AgNPs, gastrointestinal digestion of Cr-EDTA inert compound was conducted to model the simgi® dynamic transport. Monitoring chromium content in all simgi® compartments (ST, SI, AC, TC and DC) was carried out by ICP-MS. The chromium recovery percentages are shown in Fig. 3. After a single dose of Cr-EDTA (0.5 mg/mL) the maximum increase was found in the stomach and small intestine on days 1 and 2, respectively, while in the case of colon compartments (AC, TC and DC) an increase was observed between days 2 and 3. Also, of note, the operation parameters selected for gastrointestinal simulations in simgi® allowed the digestive marker to remain into the system for 48 h. Finally, no chromium was detected in any simgi® compartment at the end of the washout period (day 8). Additionally, collected simgi® samples were directly plated on different solid media to control microbiota growth during the experiment. No changes were detected for any bacterial groups evaluated (data not shown).

3.2.2. In vitro dynamic gastrointestinal digestion of GSH-AgNPs

After validating the dynamic transport, the simgi® was fed with GSH-AgNPs and their passage through the system was monitored by determining Ag concentration at the different simgi® compartments. Changes in physicochemical characteristics of AgNPs as well as changes in microbiota composition and microbial metabolic activity (ammonium production) were also evaluated during all the period.

3.2.2.1. Monitoring of silver nanoparticles by ICP-MS during the in vitro dynamic digestion process. Table 3 reports the total Ag content determined by ICP-MS in all simgi® compartments (ST, SI, AC, TC and DC) during the two gastrointestinal simulation of GSH-AgNPs (Volunteers #1 and #2). Following transition from the stomach to the colon, it was observed that, in the same way that occurred with the Cr-EDTA, the highest concentration of Ag in the stomach and small intestine was found on day 1 and 2, respectively, however, in the case of the colon compartments an increase took place on day 3. Slight differences versus theoretical data were observed, especially in the small intestine (data not shown). A similar dilution pattern in the transport of Ag along the simgi® was noticed for both volunteers. Moreover, dynamic transport of GSH-AgNPs in the simgi® was similar to that observed for the inert compound Cr-EDTA, which discarded any alterations in the intestinal fluid delivery due to the AgNPs.

3.2.2.2. Physicochemical characterisation of silver nanoparticles during the in vitro dynamic digestion process. Transmission electronic microscopy (TEM) was employed to assess the transformations (morphology and size) of the GSH-AgNPs remaining in solution during the different dynamic digestion phases. Fig. 4 displays TEM micrographs of the GSH-AgNPs. As we previously reported (García-Ruiz et al., 2015) the pristine nanoparticle samples consisted of large and polydisperse nanoparticles of ca. 10–50 nm size (Fig. 4A). A deeper analysis of the TEM sample after the obtained results showed the presence of a minor population of very small size AgNPs of ca- 3–5 nm (Fig. 4B). Fig. 5 displays representative TEM images of the content after the passage of silver nanoparticles in the stomach (Fig. 5A), ascending colon (Fig. 5B), transverse colon (Fig. 5C), and descending colon (Fig. 5D) at day 2. Regarding the small intestine samples, the analysis of several areas of the TEM sample only led to the observation of a solid residue in which nanoparticles were not detected due to transmission problems. This trend would arise from possible coagulation of the AgNPs with the organic matter present in the small intestine sample. A similar result was previously reported (Pindáková et al., 2017). As seen in the TEM analysis most AgNPs display a spherical shape of small size. This small size in the particle dimension was observed immediately after the start of digestion and was maintained throughout the whole gastrointestinal simulation process. Overall, GSH-AgNPs suspensions were dominated by particles averaging 3–5 nm in all simgi® compartments, although small populations of agglomerates of these small size nanoparticles were found, especially in ST and AC.

3.2.2.3. Changes in microbial composition during the in vitro dynamic digestion process. The effects of GSH-AgNPs on colon microbial community in the simgi® was evaluated by plate counting and qPCR. Using traditional general and selective growth media, the microbiological analysis revealed that the administration of GSH-AgNPs did not produce significant changes in most of the bacterial groups evaluated, except for total bacteria and *Lactobacillus* spp. As reflected in the plate count data of Table 3, a significant increase ($P \geq 0.05$, $\Delta\log \geq 1$) in total bacteria was observed at the end of the washout period (day 8) for both volunteers. In the case of the *Lactobacillus* spp., a significant increase over time in all compartments was noticed for volunteer #1 after GSH-AgNPs feeding.

Additionally, qPCR was used on total bacteria and the *Lactobacillus* spp. to evaluate the quantitative changes that potentially occurred in the gut microbiota composition after GSH-AgNPs feeding. As can be seen in Table 3, for the simgi® experiment with volunteer #1, a significant increase in the total bacteria was observed in the AC compartment on day 2. This increased population persisted along the studied time points. In the same line, a significant increase was noticed in the *Lactobacillus* spp. group in the AC and TC from day 3. In contrast, in the case of volunteer #2, significant changes for these groups were only detected on the last day of the washout period.

3.2.2.4. Changes in microbial activity during the in vitro dynamic digestion process. Ammonium determination is often used to characterise the proteolytic activity of intestinal microbial populations. Fig. 6 depicts the production of ammonium ion (mg NH_4^+) in simgi® colon compartments after GSH AgNPs administration. In general, for both volunteers, no large changes were observed in all colon compartments in relation to the basal levels (before GSH AgNPs feeding), which were 34.2 (AC), 250 (TC) and 194 (DC) mg NH_4^+/compartment for volunteer #1, and 119 (AC), 260 (TC) and 218 (DC) mg NH_4^+/compartment for volunteer #2. It is only worth mentioning an increase in the ammonium production in the ascending and

Table 3
Monitoring of silver nanoparticles in the simgi®. Mean values (n = 2) and standard deviation of the counts (CFU/ml) and qPCR data (log copy number/mL) for Total bacteria, *Lactobacillus* spp. and/or lactic acid bacteria after GSH-AgNPs feeding in the simgi®. The Ag concentration (μg/mL) determined by ICP-MS in the different simgi® compartments (ES: stomach; SI: small intestine; AC: ascending colon; TC: transverse colon; and DC: descending colon) is also represented.

Volunteer 1			Time (Days)					
			1	2	3	4	5	8
Log CFU/mL (Counts)	Total counts	AC	8.66 ± 0.08^{b}	8.48 ± 0.06^{ab}		8.3 ± 0.10^{a}		9.65 ± 0.12^{c}
		TC	8.45 ± 0.10^{a}	8.52 ± 0.10^{a}		8.92 ± 0.03^{b}		9.90 ± 0.08^{c}
		DC	8.10 ± 0.43^{a}	8.58 ± 0.05^{ab}		8.82 ± 0.05^{b}		9.79 ± 0.07^{c}
	Lactobacillus group	AC	3.40 ± 0.17^{a}	4.71 ± 0.02^{b}		6.95 ± .0.05^{d}		6.17 ± 0.03^{c}
		TC	4.45 ± 0.07^{a}	5.28 ± 0.18^{b}		5.87 ± 0.04^{d}		5.76 ± 0.01^{c}
		DC	3.96 ± 0.22^{a}	4.77 ± 0.13^{ab}		6.60 ± 0.07^{d}		5.35 ± 0.06^{c}
Log Copy number/mL (qPCR)	Total bacteria	AC	9.90 ± 0.04^{a}	10.91 ± 0.07^{b}	11.43 ± 0.01^{c}	10.74 ± 0.10^{b}	10.89 ± 0.04^{b}	10.95 ± 0.02^{b}
		TC	11.30 ± 0.09^{a}	11.70 ± 0.03^{c}	11.60 ± 0.03^{bc}	11.49 ± 0.09^{abc}	11.37 ± 0.02^{ab}	11.49 ± 0.05^{abc}
		DC	10.55 ± 0.09^{a}	11.17 ± 0.01^{bc}	11.48 ± 0.15^{c}	11.04 ± 0.10^{b}	11.24 ± 0.03^{bc}	11.37 ± 0.05^{c}
	Lactobacillus spp.	AC	5.41 ± 0.30^{ab}	5.43 ± 0.01^{a}	6.60 ± 0.15^{abc}	6.76 ± 0.15^{bc}	6.84 ± 0.64^{c}	7.05 ± 0.04^{c}
		TC	5.41 ± 0.06^{a}	5.67 ± 0.06^{b}	6.08 ± 0.02^{c}	6.46 ± 0.01^{d}	6.48 ± 0.04^{d}	6.45 ± 0.04^{d}
		DC	5.73 ± 0.20^{a}	5.59 ± 0.08^{a}	5.91 ± 0.04^{ab}	6.42 ± 0.02^{bc}	6.08 ± 0.20^{abc}	6.56 ± 0.21^{c}
Concentration Ag (ug Ag/mL)		ST	7.69	1.70	0.42	0.02	0.01	0.01
		SI	1.60	1.79	0.45	0.06	0.01	0.01
		AC	n.d.	1.33	1.08	0.34	0.05	0.01
		TC	n.d.	0.34	0.39	0.28	0.11	0.02
		DC	n.d.	0.10	0.35	0.28	0.16	0.03
Volunteer 2								
Log CFU/mL (Counts)	Total counts	AC	8.70 ± 0.46^{b}	8.01 ± 0.09^{a}		7.70 ± 0.04^{a}		9.57 ± 0.08^{c}
		TC	8.56 ± 0.21^{b}	7.92 ± 0.21^{a}		8.04 ± 0.09^{a}		9.57 ± 0.08^{c}
		DC	8.30 ± 0.08^{b}	7.74 ± 0.30^{a}		7.73 ± 0.04^{a}		9.66 ± 0.03^{c}
	Lactobacillus group	AC	2.23 ± 0.31	2.30 ± 0.20		2.30 ± .0.00		2.00 ± 0.00
		TC	2.62 ± 0.15	2.39 ± 0.36		2.59 ± 0.11		2.10 ± 0.17
		DC	2.98 ± 0.26^{b}	2.63 ± 0.35^{ab}		2.98 ± 0.09^{b}		2.13 ± 0.32^{a}
Log Copy number/mL (qPCR)	Total bacteria	AC	11.31 ± 0.02^{b}	11.18 ± 0.08^{ab}	11.03 ± 0.10^{a}	11.22 ± 0.05^{ab}	11.00 ± 0.01^{a}	11.33 ± 0.03^{b}
		TC	10.90 ± 0.07^{a}	11.50 ± 0.01^{d}	11.35 ± 0.03^{cd}	11.26 ± 0.03^{bc}	11.07 ± 0.11^{ab}	11.46 ± 0.01^{cd}
		DC	10.88 ± 0.01^{b}	10.88 ± 0.01^{b}	10.83 ± 0.01^{b}	10.40 ± 0.03^{ab}	10.34 ± 0.38^{ab}	9.80 ± 0.02^{a}
	Lactobacillus spp.	AC	≤4^{a}	≤4^{a}	≤4^{a}	≤4^{a}	4.28 ± 0.04^{b}	5.89 ± 0.01^{c}
		TC	≤4^{a}	≤4^{a}	≤4^{a}	≤4^{a}	≤4^{a}	5.80 ± 0.02^{b}
		DC	≤4^{a}	4.11 ± 0.38^{a}	≤4^{a}	≤4^{a}	≤4^{a}	4.73 ± 0.15^{b}
Concentration Ag (ug Ag/mL)		ST	9.28	2.29	0.54	0.04	0.03	0.04
		SI	2.01	2.46	0.58	0.25	0.10	0.06
		AC	n.d.	1.94	1.26	0.24	0.04	0.03
		TC	n.d.	0.26	0.43	0.27	0.13	0.04
		DC	n.d.	0.21	0.69	0.65	0.51	0.08

*For given bacterial groups (counts or qPCR data), different letters show significant differences according to the Tukey's test ($p < 0.05$).

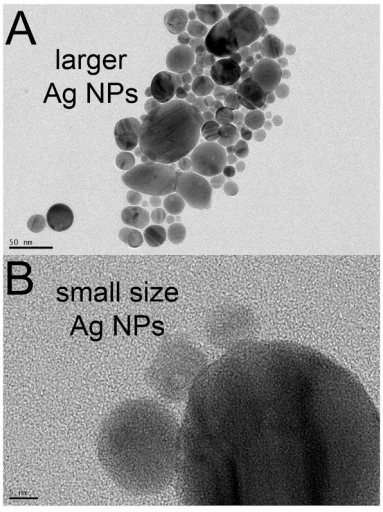

Fig. 4. Representative TEM images of pristine GSH-AgNPs populations of nanoparticles of ca. 10–50 nm (A) and very small nanoparticles of ca. 3–5 nm size (B).

transverse colon at the end of the washout period for both volunteers. In contrast, in the case of descending colon, the administration of GSH AgNPs resulted in a decrease in ammonium production for volunteer #1 and an increase in volunteer #2.

As expected, the ammonium production was colon-compartment dependent, being higher in descending and transverse colon than in the ascending colon.

4. Discussion

For ethical, regulatory, and economic reasons, different *in vitro* human digestion models have been developed as an alternative to *in vivo* assays. Simgi® is a multi-compartment dynamic model that allows simulation of the complex evolution over time of the main physicochemical and mechanical phenomena during digestion and offering simple access to the different parts of the digestive tract, giving instant information about the fate of compounds in the gastrointestinal environment (Dupont et al., 2018). The studies carried out so far have shown the suitability of the model to carry out dynamic gastric digestion (Miralles et al., 2018) and colon fermentative process (Barroso et al., 2015; Cueva et al., 2015; Gil-Sánchez et al., 2018). However, the design of a system also allows a joint simulation with all simgi® compartments, that is, the stomach, small intestine, ascending, transverse and descending colon. The transit through these compartments is

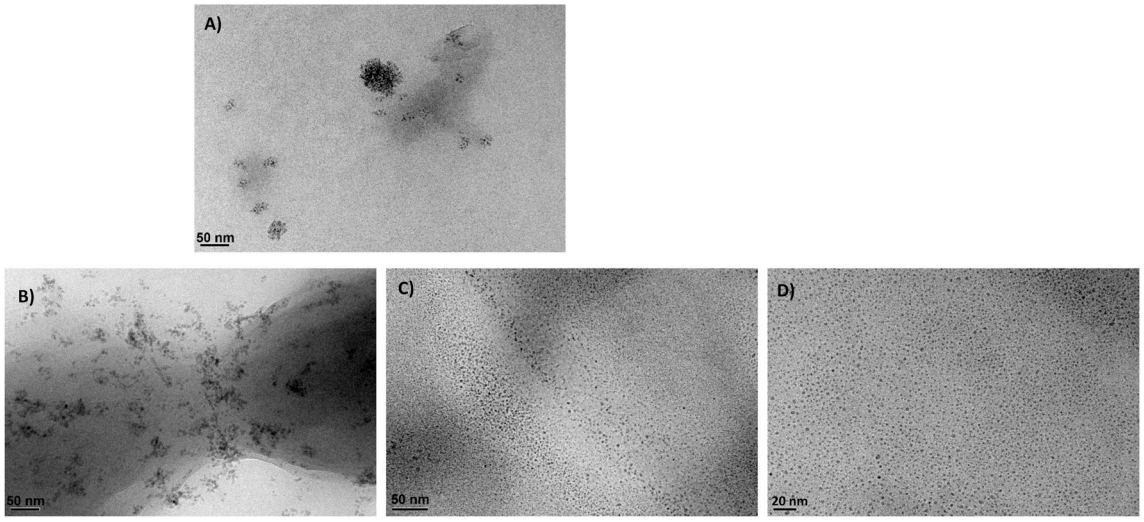

Fig. 5. TEM images of GSH-AgNPs after digestion in the stomach (A), ascending colon (B), transverse colon (C) and descending colon (D).

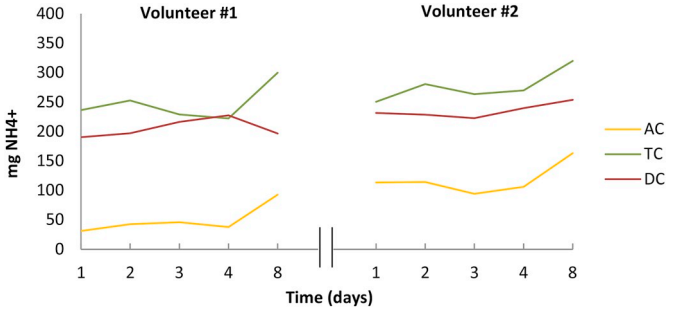

Fig. 6. The quantity of ammonium ion (mg NH_4^{+}) in ascending colon (AC), transverse colon (TC) and descending colon (DC) after GSH AgNPs administration. For both volunteers, ammonium ion determinations were carried out in duplicate (n = 2): the day of the feeding (day 1) and during washout period (days 2, 3, 4, 5 and 8).

crucial for digestion and absorption of nutrients (Müller et al., 2018). Considering this, our study was focused on the evaluation of the dynamic fluid transport through all simgi® compartments by a gastrointestinal simulation of an inert compound (resistant to degradation by human gut bacterial enzymes), Cr-EDTA. This type of compound is commonly used to validate the operation of *in vitro* and *in vivo* models (Barbé et al., 2013; Chiang et al., 2008). The results of this study showed that the maximum levels of Cr-EDTA in the different simgi® compartments were reached sequentially along digestion process progression, therefore the compound evidently remains in the system for 48 h, which is compliant with a physiological reality (Aulton and Taylor, 2018). In addition, no traces of chromium were detected in any samples of the simgi® compartments at the end of the washout period, reflecting the return to initial conditions within 8 days. This period was slightly higher than the one used with SHIME® model with caffeine (6 days) (van Dorsten et al., 2012), which could be due to the different design of the stomach and the gastric parameters used (Barroso et al., 2015; Van de Wiele et al., 2015). In this sense, the main advantage of the gastric simgi® compartment is its distinctive technical features that allow the peristaltic mixing movements and controlled emptying according to the Elashoff equation (Miralles et al., 2018) which in turn enables the modification of different settings according to physiological conditions (i.e. type of food, drug, age, health status, etc.). This versatility of simgi® makes it an excellent model for a wide variety of applications across multiple disciplines, including nanotechnology. In addition, cultured bacterial counts showed that the viability of the main bacterial groups present in the colon regions was not altered by exposure to Cr-EDTA complex (data not shown).

Silver nanoparticles have become one of the most in-demand nanoparticles in different sectors (textiles, food, consumer products, medicine) owing to their unique physical and chemical characteristics along with their antimicrobial ability (Akter et al., 2018). However, little is known about the diversified mechanisms and action of the cytotoxicity of AgNPs, as well as their short- or long-term exposure outcomes on human physiology (Mishra et al., 2016; Nel et al., 2006). In this context, novel and recent applications of AgNPs have been introduced to the field of food production. In particular, AgNPs has been proposed as a new alternative to replace or complement the antiseptic properties of SO_2 owing to the potential risks of sulphites to human health (García-Ruiz et al., 2015; Gil-Sánchez et al., 2019). Also, the antimicrobial effectiveness of GSH-AgNPs against multidrug-resistant (MDR) *Campylobacter* strains isolated from the chicken food chain and clinical patients has been proved at low GSH-AgNPs concentrations (Silvan et al., 2018). In turn, the morphological changes and toxicity of GSH-AgNPs have been recently examined after *in vitro* three step digestion (oral, gastric and intestinal phases) (Gil-Sánchez et al., 2019). At the end of the digestion process, the size and shape of the nanoparticles remained almost unaltered. Finally, Caco-2 cell experiments seemed to exclude toxicity of these AgNPs at the intestinal epithelium (Gil-Sánchez et al., 2019). Overall, these studies provide preliminary information about the food applications and health properties of AgNPs, however, a major research initiative is needed to assess their effects on intestinal microbiota and host health.

Dynamic gastrointestinal digestion simulators are considered new *in vitro* strategies for evaluating the changes in food and consumer products during their transit through the gastrointestinal tract, as well as for determining possible changes in the composition and functionality of the intestinal microbiota because of food ingestion (Thuenemann, 2015). To the best of our knowledge, the *in vitro* intestinal digestion of AgNPs has not been investigated before, using a dynamic gastrointestinal digestion simulator.

Our first approach to the study of the effects of AgNPs on intestinal microbiota in static experiments proved non-significant changes in the bacteria population for both nanoparticles (PEG-20 AgNPs and GSH-AgNPs). Based on these early results, and those obtained from previous studies for GSH-AgNPs, such as an effective antimicrobial activity against foodborne pathogens (Silván et al., 2018) as well as wine-related microorganisms (Gil-Sánchez et al., 2019), a good maintenance of the size and shape of the nanoparticles during preliminary *in vitro* digestion (Gil-Sánchez et al., 2019), the absence of toxicity against intestinal epithelium (Caco-2 cell experiments) (Gil-Sánchez et al., 2019),

and a better solubility in the nutritive medium used in the simgi than PEG-AgNPs 20, led us to select these nanoparticles to perform *in vitro* dynamical gastrointestinal digestion in the simgi®. Regarding the monitoring of silver content in simgi® results displayed that the dynamic transport of nanoparticles was very similar to that observed in the inert compound, demonstrating the suitability of the chosen gastrointestinal parameters. A similar dilution pattern in the transport of Ag along the simgi® was also noticed for both volunteers confirming the reproducibility of the model. On the other hand, slight differences between practical and theoretical Ag concentration in simgi® samples were observed. The effect of important parameters in physiological solutions such as pH, salt and enzyme contents cannot be discarded (Axson et al., 2015; Pindáková et al., 2017). Nevertheless, other physicochemical properties of silver nanoparticles such as the particle size and the coating material could also play a vital role in the behaviour of AgNPs in the gastrointestinal tract (Akter et al., 2018). In fact, the TEM analysis proved that the digested samples comprised AgNPs displaying a spherical shape and a very small size. In comparison with pristine GSH-AgNPs, the size of the digested nanomaterials would correspond with the minor population of small size AgNPs detected in the GSH-AgNPs sample (Fig. 5). We speculate that the larger size AgNPs observed before digestion would be precipitated in the centrifugation and filtration of the samples prior to TEM sampling. This small size in the particle dimension was observed immediately after the start of digestion and was maintained throughout the whole gastrointestinal simulation process. The analysis of the GSH-AgNPs dispersions samples through TEM showed that they were mainly composed of particles averaging 3–5 nm in all simgi® compartments. In some specific samples (stomach and AC) a small population of agglomerates of these small size nanoparticles was found. Therefore, the TEM analysis suggests that the smallest AgNPs are still dispersed in the fluids of the gastrointestinal juices along the whole simulation process. The AgNPs underwent several transformations, including their simultaneous dispersion and slight agglomeration in gastrointestinal fluids.

Speaking about the effects of AgNPs on intestinal microbiota, microbiological counts revealed that the GSH-AgNPs feeding led to a significant increase in total bacteria at the end of the washout period for both volunteers, which could be due to AgNPs washing effect. In the case of the *Lactobacillus* spp. group, a gradual significant increase in all compartments was noticed for volunteer #1 after GSH-AgNPs feeding. Conversely, data of qPCR analysis showed that the GSH-AgNPs lead to a significant increase in *Lactobacillus* spp. which was day-, individual- and compartment-dependent. According to this finding, other studies have revealed the increment of gut *Lactobacillaceae* family after the treatment with AgNPs (Han et al., 2014; van den Brule et al., 2016). Additionally, a study performed in mice, based on the 16S rRNA sequencing of intestinal microbiota, reported that animals exposed to different AgNPs during 28 days (oral dosing 10 mg/kg/day) showed no effects on the microbiota composition (Wilding et al., 2016). Another previous experiment that measured cecal bacterial phyla found that four-week-old rats exposed to varying doses of AgNPs did not reveal any differences relative to controls (Hadrup et al., 2012). Furthermore, Catto et al. (2019) did not observe changes in the core faecal microflora and its SCFAs profiles after in-vitro exposure of 1 μgml-1 AgNPs in faecal fermentation cultures. By contrast, in zebrafish, feeding of diets laced with AgNPs (500 mg/kg food for 14 days) changed the composition of the intestinal microbiome (Merrifield et al., 2013). Das et al. (2014) examined the effects of 48 h exposure to AgNPs (25, 100, and 200 mg/L) on a defined bacterial community established from a healthy human donor. Their findings also revealed that these nanomaterials induced a shift towards more pathogenic bacterial species. In addition, Williams et al. (2015) evaluated the effects of sub-chronic exposure of silver nanoparticles (9, 18 and 36 mg/kg body weight) on Sprague-Dawley rat intestinal microbiota for 13 weeks. The results produced an apparent shift in the gut microbiota toward greater proportions of Gram-negative bacteria. In general, these conflicting results on the silver nanoparticles effects on intestinal microbiota seem to be due to, in part, the differences in size of nanoparticle, presence or absence of stabilising agents, duration of exposure, and doses administrated among other factors (Mercier-Bonin et al., 2016; Pietroiusti et al., 2016).

In terms of metabolic activity, the exposure to silver nanoparticles did not produce large changes in the ammonium production by intestinal microbiota. As expected, the ammonium production was colon-compartment dependent, being higher in the descending and transverse colon, than in ascending colon which is in accordance with previous studies performed in the simgi® (Cueva et al., 2015; Gil-Sánchez et al., 2018). Additionally, a specific increase in the ammonium levels occurs at the end of wash out period which could be related with the significant increase in *Lactobacillus* group, which is able to produce this metabolite by amino acid deamination (Scott et al., 2013).

5. Conclusions

In summary, this study illustrates, for the first time, the use of a robust and consistent model system for validate the fluid dynamic transport through all simgi® compartments. Furthermore, this work has included the development of the complete operation of the dynamic gastrointestinal simulator, simgi®, which has proven to be a useful tool for assessing the behaviour of AgNPs in physiological conditions. Dynamic transport of nanoparticles was very similar to that observed in the inert digestive compound Cr-EDTA, demonstrating the suitability of the chosen gastrointestinal parameters. A similar dilution pattern in the transport of Ag along the simgi® was also noticed for both volunteers confirming the reproducibility of the model. The AgNPs underwent several transformations in gastrointestinal fluids and seems to expose the intestine in forms that were structurally different from the original forms. Overall, no changes in bacterial composition or ammonium ion production were observed during the dynamic gastrointestinal simulations of AgNPs in the simgi®. This appears to confirm that these nanomaterials did not disturb the composition and metabolic activity of human intestinal microbiota, which is of great interest in view of its potential application in the food field.

Declaration of interests

The authors declare that they have no known competing financial interests or personal relationships that could have appeared to influence the work reported in this paper.

Acknowledgements

This work was carried out with the financial support of the Spanish Ministry of Science, Innovation and Universities (PRI-PIBAR-2011-1358, AGL2015-64522-C2-1 projects), and the Comunidad de Madrid Program (ALIBIRD-CM S2013/ABI-2728; ALIBIRD-CM 2020 P2018/BAA-4343). I. G-S is the recipient of fellowship from the Spanish FPU-MECD (FPU14/05760) programme.

Transparency document

Transparency document related to this article can be found online at https://doi.org/10.1016/j.fct.2019.110657.

References

Akter, M., Sikder, M.T., Rahman, M.M., Ullah, A.K.M.A., Hossain, K.F.B., Banik, S., ... Kurasaki, M., 2018. A systematic review on silver nanoparticles-induced cytotoxicity: physicochemical properties and perspectives. J. Adv. Res. 9, 1–16. https://doi.org/10.1016/j.jare.2017.10.008.

Aulton, M.E., Taylor, M.G., 2018. Aulton's Pharmaceutics: the Design and Manufacture of Medicines, 4 ed. Elsevier Health Sciences.

Axson, J.L., Stark, D.I., Bondy, A.L., Capracotta, S.S., Maynard, A.D., Philbert, M.A., ... Ault, A.P., 2015. Rapid kinetics of size and pH-dependent dissolution and aggregation

of silver nanoparticles in simulated gastric fluid. J. Phys. Chem. 119, 20632–20641. https://doi.org/10.1021/acs.jpcc.5b03634.
Balcaen, L., Bolea-Fernandez, E., Resano, M., Vanhaecke, F., 2015. Inductively coupled plasma – tandem mass spectrometry (ICP-MS/MS): a powerful and universal tool for the interference-free determination of (ultra)trace elements – a tutorial review. Anal. Chim. Acta 894, 7–19. https://doi.org/10.1016/j.aca.2015.08.053.
Barbé, F., Ménard, O., Le Gouar, Y., Buffière, C., Famelart, M., Laroche, B., ... Rémond, D., 2013. The heat treatment and the gelation are strong determinants of the kinetics of milk proteins digestion and of the peripheral availability of amino acids. Food Chem. 136, 1203–1212. https://doi.org/10.1016/j.foodchem.2012.09.022.
Barroso, E., Cueva, C., Peláez, C., Martínez-Cuesta, M.C., Requena, T., 2015. The computer-controlled multicompartmental dynamic model of the gastrointestinal system SIMGI. In: Verhoeckx, K., Cotter, P., López-Expósito, I., Kleiveland, C., Lea, T., Mackie, A., Requena, T., Swiatecka, D., Wichers, H. (Eds.), The Impact of Food Bioactives on Health: in Vitro and Ex Vivo Models. Springer International Publishing, Cham, pp. 319–327.
Brouwers, J., Anneveld, B., Goudappel, G., Duchateau, G., Annaert, P., Augustijns, P., Zeijdner, E.E., 2011. Food-dependent disintegration of immediate release fosamprenavir tablets: in vitro evaluation using magnetic resonance imaging and a dynamic gastrointestinal system. Eur. J. Pharm. Biopharm. 77, 313–319. https://doi.org/10.1016/j.ejpb.2010.10.009.
Catto, C., Garuglieria, E., Borrusob, L., Erba, D., Casiraghi, M.C., Cappitelli, F., et al., 2019. Impacts of dietary silver nanoparticles and probiotic administrationon the microbiota of an in-vitro gut model. Environ. Pollut. 245, 754–763. https://doi.org/10.1016/j.envpol.2018.11.019.
Cueva, C., Jiménez-Girón, A., Muñoz-González, I., Esteban-Fernández, A., Gil-Sánchez, I., Dueñas, M., ... Moreno-Arribas, M.V., 2015. Application of a new Dynamic Gastrointestinal Simulator (SIMGI) to study the impact of red wine in colonic metabolism. Food Res. Int. 72, 149–159. https://doi.org/10.1016/j.foodres.2015.03.003.
Chaudhry, Q., Scotter, M., Blackburn, J., Ross, B., Boxall, A., Castle, L., ... Watkins, R., 2008. Applications and implications of nanotechnologies for the food sector. Food Addit. Contam. A 25, 241–258. https://doi.org/10.1080/02652030701744538.
Chiang, C.C., Croom, J., Chuang, S.T., Chiou, P.W.S., Yu, B., 2008. Development of a dynamic system simulating pig gastric digestion. Asian-Australas. J. Anim. Sci. 21, 1522–1528. https://doi.org/10.5713/ajas.2008.70640.
Das, P., McDonald, J., Petrof, E.O., Allen-Vercoe, E., Walker, V.K., 2014. Nanosilver-mediated change in human intestinal microbiota. Nanotechnology 5. https://doi.org/10.4172/2157-7439.1000235.
Dupont, D., Alric, M., Blanquet-Diot, S., Bornhorst, G., Cueva, C., Deglaire, A., Van den Abbeele, P., 2018. Can dynamic in vitro digestion systems mimic the physiological reality? Crit. Rev. Food Sci. Nutr. 23, 1–17. https://doi.org/10.1080/10408398.2017.1421900.
Elashoff, J.D., Reedy, T.J., Meyer, J.H., 1982. Analysis of gastric emptying data. Gastroenterology 83, 1306–1312. https://doi.org/10.1016/S0016-5085(82)80145-5.
García-Ruiz, A., Crespo, J., López-de-Luzuriaga, J.M., Olmos, M.E., Monge, M., Rodríguez-Álfaro, M.P., ... Moreno-Arribas, M.V., 2015. Novel biocompatible silver nanoparticles for controlling the growth of lactic acid bacteria and acetic acid bacteria in wines. Food Control 50, 613–619. https://doi.org/10.1016/j.foodcont.2014.09.035.
Gil-Sánchez, I., Cueva, C., Sanz-Buenhombre, M., Guadarrama, A., Moreno-Arribas, M.V., Bartolomé, B., 2018. Dynamic gastrointestinal digestion of grape pomace extracts: bioaccessible phenolic metabolites and impact on human gut microbiota. J. Food Compos. Anal. 68, 41–52. https://doi.org/10.1016/j.jfca.2017.05.005.
Gil-Sánchez, I., Monge, M., Miralles, B., Armentia, G., Cueva, C., Crespo, J., et al., 2019. Some new findings on the potential use of biocompatible silver nanoparticles in winemaking. Innov. Food Sci. Emerg. Technol. 51, 64–72. https://doi.org/10.1016/j.ifset.2018.04.017.
Guerra, A., Etienne-Mesmin, L., Livrelli, V., Denis, S., Blanquet-Diot, S., Alric, M., 2012. Relevance and challenges in modeling human gastric and small intestinal digestion. Trends Biotechnol. 30, 591–600. https://doi.org/10.1016/j.tibtech.2012.08.001.
Hadrup, N., Loeschner, K., Bergstrom, A., Wilcks, A., Gao, X., Vogel, U., 2012. Subacute oral toxicity investigation of nanoparticulate and ionic silver in rats. Arch. Toxicol. 86, 543–551. https://doi.org/10.1007/s00204-011-0759-1.
Han, X., Geller, B., Moniz, K., Das, P., Chippindale, A.K., Walker, V.K., 2014. Monitoring the developmental impact of copper and silver nanoparticle exposure in Drosophila and their microbiomes. Sci. Total Environ. 487, 822–829. https://doi.org/10.1016/j.scitotenv.2013.12.129.
Joly, C., Gay-Quéheillard, J., Léké, A., Chardon, K., Delanaud, S., Bach, V., Khorsi-Cauet, H., 2013. Impact of chronic exposure to low doses of chlorpyrifos on the intestinal microbiota in the Simulator of the Human Intestinal Microbial Ecosystem (SHIME®) and in the rat. Environ. Sci. Pollut. Control Ser. 20, 2726–2734. https://doi.org/10.1007/s11356-012-1283-4.
Kästner, C., Lichtenstein, D., Lampen, A., Thünemann, A.F., 2017. Monitoring the fate of small silver nanoparticles during artificial digestion. Physicochem. Eng. Asp. 526, 76–81.
Kong, F., Singh, R.P., 2008. Disintegration of solid foods in human stomach. J. Food Sci. 73, R67–R80. https://doi.org/10.1111/j.1750-3841.2008.00766.x.
Lefebvre, D.E., Venema, K., Gombau, L., Valerio, L.G., Raju, J., Bondy, G.S., ... Stone, V., 2015. Utility of models of the gastrointestinal tract for assessment of the digestion and absorption of engineered nanomaterials released from food matrices. Nanotoxicology 9, 523–542. https://doi.org/10.3109/17435390.2014.948091.
Lucas-González, R., Viuda-Martos, M., Pérez-Alvarez, J.A., Fernández-López, J., 2018. *In vitro* digestion models suitable for foods: opportunities for new fields of application and challenges. Food Res. Int. 107, 423–436. https://doi.org/10.1016/j.foodres.2018.02.055.
Ménard, O., Cattenoz, T., Guillemin, H., Souchon, I., Deglaire, A., Dupont, D., Picque, D., 2014. Validation of a new in vitro dynamic system to simulate infant digestion. Food Chem. 145, 1039–1045. https://doi.org/10.1016/j.foodchem.2013.09.036.
Mercier-Bonin, M., Despax, B., Raynaud, P., Houdeau, E., Thomas, M., 2016. Oral exposure and fate of food nanoparticles within the gut: examples of silver and titanium dioxide. Cah. Nutr. Diet. 51, 195–203.
Mercier-Bonin, M., Despax, B., Raynaud, P., Houdeau, E., Thomas, M., 2018. Mucus and microbiota as emerging players in gut nanotoxicology: the example of dietary silver and titanium dioxide nanoparticles. Crit. Rev. Food Sci. Nutr. 58, 1023–1032. https://doi.org/10.1080/10408398.2016.1243088.
Merrifield, D.L., Shaw, B.J., Harper, G.M., Saoud, I.P., Davies, S.J., Handy, R.D., Henry, T.B., 2013. Ingestion of metal-nanoparticle contaminated food disrupts endogenous microbiota in zebrafish (Danio rerio). Environ. Pollut. 174, 157–163. https://doi.org/10.1016/j.envpol.2012.11.017.
Meunier, J.P., Manzanilla, E.G., Anguita, M., Denis, S., Pérez, J.F., Gasa, J., ... Alric, M., 2008. Evaluation of a dynamic in vitro model to simulate the porcine ileal digestion of diets differing in carbohydrate composition1. J. Anim. Sci. 86, 1156–1163. https://doi.org/10.2527/jas.2007-0145.
Minekus, M., Alminger, M., Alvito, P., Ballance, S., Bohn, T., Bourlieu, C., ... Brodkorb, A., 2014. A standardised static in vitro digestion method suitable for food - an international consensus. [10.1039/C3FO60702J]. Food Funct. 5, 1113–1124. https://doi.org/10.1039/C3FO60702J.
Minekus, M., Smeets-Peeters, M., Bernalier, A., Marol-Bonnin, S., Havenaar, R., Marteau, P., ... Huis in't Veld, J.H., 1999. A computer-controlled system to simulate conditions of the large intestine with peristaltic mixing, water absorption and absorption of fermentation products. Appl. Microbiol. Biotechnol. 53, 108–114. https://doi.org/10.1007/s002530051622.
Miralles, B., del Barrio, R., Cueva, C., Recio, I., Amigo, L., 2018. Dynamic gastric digestion of a commercial whey protein concentrate. J. Sci. Food Agric. 98, 1873–1979. https://doi.org/10.1002/jsfa.8668.
Mishra, A.R., Zheng, J., Tang, X., Goering, P.L., 2016. Silver nanoparticle-induced autophagic-lysosomal disruption and NLRP3-inflammasome activation in HepG2 cells is size-dependent. Toxicol. Sci. 150, 473–487. https://doi.org/10.1093/toxsci/kfw011.
Monge, M., Moreno-Arribas, M.V., 2016. Applications of nanotechnology in wine production and quality and safety control. In: Moreno-Arribas, M.V., Bartolomé Suáldea, B. (Eds.), Wine Safety, Consumer Preference, and Human Health. Springer International Publishing, pp. 51–69.
Müller, M., Canfora, E.E., Blaak, E.E., 2018. Gastrointestinal transit time, glucose homeostasis and metabolic health: modulation by dietary fibers. Nutrients 10, 275. https://doi.org/10.3390/nu10030275.
Nel, A., Xia, T., Mädler, L., Li, N., 2006. Toxic potential of materials at the nanolevel. Science 311, 622–627. https://doi.org/10.1126/science.1114397.
Pietroiusti, A., Magrini, A., Campagnolo, L., 2016. New frontiers in nanotoxicology: gut microbiota/microbiome-mediated effects of engineered nanomaterials. Toxicol. Appl. Pharmacol. 15 (299), 90–95. https://doi.org/10.1016/j.taap.2015.12.017.
Pindáková, L., Kašpárková, V., Kejlová, K., Dvořáková, M., Krsek, D., Jírová, D., Kašparová, L., 2017. Behaviour of silver nanoparticles in simulated saliva and gastrointestinal fluids. Int. J. Pharm. 527, 12–20. https://doi.org/10.1016/j.ijpharm.2017.05.026.
Ramos, K., Ramos, L., Gómez-Gómez, M.M., 2017. Simultaneous characterisation of silver nanoparticles and determination of dissolved silver in chicken meat subjected to in vitro human gastrointestinal digestion using single particle inductively coupled plasma mass spectrometry. Food Chem. 221, 822–828. https://doi.org/10.1016/j.foodchem.2016.11.091.
Scott, K.P., Gratz, S.W., Sheridan, P.O., Flint, H.J., Ducan, S.H., 2013. Influence of diet on the gut microbiota. Pharmacol. Res. 69, 52–60.
Sergeevna, A.S., Anatolevich, S.O., Nurchallaeva, S.G., Aleksandrovich, B.A., Petrovich, R.E., Vladimirovich, S.S., et al., 2018. Silver in the meat and organs of broiler chickens in case of using colloidal silver as an alternative to antibiotics. Biometals 31 (6), 975–980.
Silvan, J.M., Zorraquin-Peña, I., Gonzalez de Llano, D., Moreno-Arribas, M.V., Martinez-Rodriguez, A.J., 2018. Antibacterial activity of glutathione-stabilized silver nanoparticles against *Campylobacter* multidrug-resistant strains. Front. Microbiol. 9, 458. https://doi.org/10.3389/fmicb.2018.00458.
Sun, G., Van de Wiele, T., Alava, P., Tack, F.M.G., Du Laing, G., 2017. Bioaccessibility of selenium from cooked rice as determined in a simulator of the human intestinal tract (SHIME). J. Sci. Food Agric. 97, 3540–3545. https://doi.org/10.1002/jsfa.8208.
Tamargo, A., Gil-Sánchez, I., Miralles, B., Martín, D., Rodríguez-Risco, M., Fornari, T., Bartolomé, B., Moreno-Arribas, M.V., Cueva, C., 2017. The dynamic gastrointestinal simulator (Simgi®): a useful tool for clinical nutrition. Nutr. Hosp. 34, 1489–1496. https://doi.org/10.20960/nh.1207.
Thuenemann, E.C., 2015. Dynamic digestion models: general introduction. In: Verhoeckx, K., Cotter, P., López-Expósito, I., Kleiveland, C., Lea, T., Mackie, A., Requena, T., Swiatecka, D., Wichers, H. (Eds.), The Impact of Food Bioactives on Health: in Vitro and Ex Vivo Models, pp. 33–36.
Van de Wiele, T., Van den Abbeele, P., Ossieur, W., Possemiers, S., Marzorati, M., 2015. The simulator of the human intestinal microbial ecosystem (SHIME®). In: Verhoeckx, K., Cotter, P., López-Expósito, I., Kleiveland, C., Lea, T., Mackie, A., Requena, T., Swiatecka, D., Wichers, H. (Eds.), The Impact of Food Bioactives on Health: in Vitro and Ex Vivo Models, pp. 305–317.
van den Brule, S., Ambroise, J., Lecloux, H., Levard, C., Soulas, R., De Temmerman, P., ... Lison, D., 2016. Dietary silver nanoparticles can disturb the gut microbiota in mice. Part. Fibre Toxicol. 13, 38. https://doi.org/10.1186/s12989-016-0149-1.
van Dorsten, F.A., Peters, S., Gross, G., Gomez-Roldan, V., Klinkenberg, M., de Vos, R.C., ... Jacobs, D.M., 2012. Gut microbial metabolism of polyphenols from black tea and red wine/grape juice is source-specific and colon-region dependent. J. Agric. Food

Chem. 60, 11331–11342. https://doi.org/10.1021/jf303165w.
Walczak, A.P., Fokkink, R., Peters, R., Tromp, P., Herrera Rivera, Z.E., Rietjens, I.M.C.M., ... Bouwmeester, H., 2012. Behaviour of silver nanoparticles and silver ions in an in vitro human gastrointestinal digestion model. Nanotoxicology 7, 1198–1210. https://doi.org/10.3109/17435390.2012.726382.
Wijnhoven, S.W.P., Peijnenburg, W.J.G.M., Herberts, C.A., Hagens, W.I., Oomen, A.G., Heugens, E.H.W., ... Geertsma, R.E., 2009. Nano-silver – a review of available data and knowledge gaps in human and environmental risk assessment. Nanotoxicology 3 (2), 109–138. https://doi.org/10.1080/17435390902725914.
Wilding, L.A., Bassis, C.M., Walacavage, K., Hashway, S., Leroueil, P.R., Morishita, M., ... Bergin, I.L., 2016. Repeated dose (28 day) administration of silver nanoparticles of varied size and coating does not significantly alter the indigenous murine gut microbiome. Nanotoxicology 10 (5), 513–520. https://doi.org/10.3109/17435390.2015.1078854.
Williams, K., Milner, J., Boudreau, M.D., Gokulan, K., Cerniglia, C.E., Khare, S., 2015. Effects of subchronic exposure of silver nanoparticles on intestinal microbiota and gut-associated immune responses in the ileum of Sprague-Dawley rats. Nanotoxicology 9, 279–289. https://doi.org/10.3109/17435390.2014.921346.
Yin, N., Cai, X., Chen, X., Du, H., Xu, J., Wang, L., ... Cui, Y., 2017. Investigation of bioaccessibility of Cu, Fe, Mn, and Zn in market vegetables in the colon using PBET combined with SHIME. Sci. Rep. 7 (17578). https://doi.org/10.1038/s41598-017-17901-1.
Zuluaga, J., Rodríguez, N., Rivas-Ramirez, I., de la Fuente, V., Rufo, L., Amils, R., 2011. An improved semiquantitative method for elemental analysis of plants using inductive coupled plasma mass spectrometry. Biol. Trace Elem. Res. 144, 1302–1317. https://doi.org/10.1007/s12011-011-9140-8.